Effect of Friction Stir Welding on Microstructure of a 5024 Alloy

Diana Yuzbekova[*], Vladislav Kulitskiy, Anna Mogucheva,
Rustam Kaibyshev

Belgorod State University, Pobeda 85, Belgorod 308015, Russia

Abstract. Influence of friction stir welding (FSW) on microstructure of an Al-4.57Mg-0.35Mn-0.2Sc-0.09Zr (wt. pct.) alloy was studied. Following parameters of FSW were used: the rotation speeds of 500, 650 and 800 rpm, the traverse speed of 75 mm/min and the tilt angle of 2.5°. Defect-free welds were obtained using all these parameters. FSW leads to the formation of fully recrystallized microstructures with average grain sizes less 2 μm and a moderate dislocation density of ~10^{13} m^{-2} in the stir zone. No evidence for abnormal grain growth was found in the heat affected zone of the weld. The nano-scale Al$_3$(Sc,Zr) dispersoids coarsened to 21 nm but retained coherent interfaces and cube-cube orientation relationship with the matrix.

Introduction

It is well known that severe plastic deformation (SPD) is the universal and most common methods of grain refinement in aluminium alloys [1]. SPD by using friction stir welding/processing (FSW/FSP) provides attractive opportunity for extensive grain refinement in aluminum alloys containing a dispersion of nanoscale particles [2-5]. Under FSW a rotating tool is pressed between two abutting or overlapping plates [5,6]. Heat is generated, principally due to friction of shoulder pressed to two plates that provides softening in a zone with dimension slightly higher than a shoulder diameter [5,6]. As the tool is traversed along the joint line, material is swept around the pin between the retreating side (RS) of the tool and the surrounding un-deformed material [5,6]. The weld is formed by SPD of a material at temperatures below the melting temperature. The peak temperature during FSW of aluminum alloys is believed to remain below ~500°C [5,7]. The microstructures evolved during FSW in none-age harden able aluminum alloys is different from those obtained by other SPD techniques by a very high portion of high-angle boundaries (HAB) ≥90 pct and entirely random texture [2,3]. The grains in stir zone (SZ) exhibit equiaxed shape, and contain relatively low dislocation density [2,3]. Moreover FSW has shown potential to produce UFG microstructure with more than 90 pct. high-angle grain boundaries (HAGBs) [1,2]. FSW has proven to a very effective severe plastic deformation technique because of unique combination of high strain, high strain rate and high processing temperature [1-6].

It is known that Al-Mg alloys with ultra-fine grained (UFG) structures produced by SPD exhibit superior mechanical properties. The minor additions of Sc and Zr in Al-Mg alloys give rise to the precipitation of coherent nano-scale Al$_3$(Sc,Zr) dispersoids, which impart significant strengthening effect and promote efficiency of extensive grain refinement [3,5,8]. However the experimental data on the effect of FSW on Al$_3$(Sc,Zr) dispersoids are very limited and contradictory. The aim of this study is investigation of FSW effect on the microstructure and Al$_3$(Sc,Zr) dispersoids in Al-Mg-Sc-Zr alloy.

Experimental material and procedure

The 5024 alloy with a chemical composition of Al-4.57Mg-0.35Mn-0.2Sc-0.09Zr (in wt. pct.) was produced by continuous casting [9]. Then solution treatment was carried out at 370±10°C for 12 h. Next, the ingot was extruded at a temperature of 380°C with a reduction of ~70 pct [9]. Then the samples were machined from the central part of the extruded billet parallel to the extrusion direction into plates with thickness of 2.3 mm, length of 80 mm and width of 42 mm. These plates were butt-welded parallel to the extrusion direction using the FSW. The tool was fabricated from

tool steel and consisted of a shoulder with a diameter of 12.5 mm and a M5 cylindrical pin, which was 2.05 mm in length. FSW was performed using an AccuStir 1004 machine at tool rotational speeds of 500, 650 and 800 rpm and a tool travel speed of 75 mm/min. During FSW, the tool was tilted by 2.5° from the sheet normal such that the rear of the tool was lower than the front. The principal directions of the welding geometry are denoted throughout this study as the welding direction (WD), the transversal direction (TD) and the normal direction (ND) of the welded sheets. Other details of FSW processing were described elsewhere [3].

The microstructure of material was studied using optical microscopy (Olympus GX71), transmission electron microscopy (TEM, Jeol–2100) and scanning electron microscopy (SEM, Quanta 600). All of this technique was described in previous papers in details [9].

Results and Discussion

Friction stir welds. Figure 1 shows low-magnification optical images of transversal cross-sections of friction-stir welds obtained with different tool rotation speeds. There is no evidence for volumetric defects in the welds. This result confirms that using all three parameters of the welding is feasible to produce defect-free welds. A distinct SZ could be recognized in each weld. In this zone the distinct flow patterns located in asymmetrical way relative to the weld center line comprise well-known onion-ring structure [5]. Almost homogeneous UFG structure is observed within the SZs.
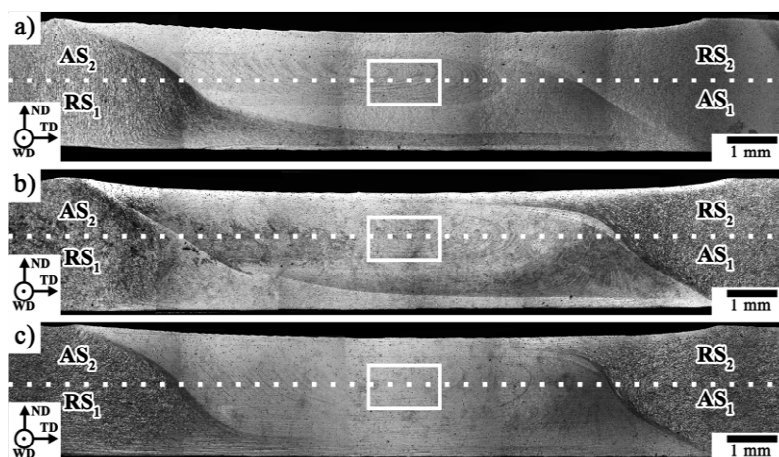

Fig. 1. The microstructure of 5024 alloy after FSW with tool rotation speed of (a) 500 rpm, (b) 650 rpm, (c) 800 rpm

Microstructure in initial condition and after FSW. The microstructure of the 5024 alloy after extrusion is characterized by a bimodal distribution of the grain size (Fig. 2(a)) [9]. The size of coarse grains was 200 and 20 μm in longitudinal and transverse directions, respectively, and the average size of fine grains was 2 μm (Fig. 2(a)). Electron backscatter diffraction (EBSD) confirms the uniformity of the recrystallized structure and the lacking of remnants of unrecrystallized grains (Fig. 2(a-c)). Fig. 2(b-d) shows the EBSD maps taken from the central parts of the stir zones produced with different tool rotation speed (the location of the microstructural observations is indicated in Fig. 1). Table 1 summarizes the relevant microstructural characteristics. The tool rotation speeds of 500, and 650 produce microstructures with an average grain size of 1.5, portion of HABs ~90° an average misorientation is ~38° 1.5 and 2.0 μm, respectively. The grains are completely separated by HABs (Fig. 2(b-d)). Grain-boundary misorientation distribution after FSW is shown in Fig. 2(b'-d'). The HABs fraction was near 90 pct. after all FSW regimes (Fig. 2(b'-d'), Table 1). Average misorientation is close to 40.7°, predicted by Mackenzie for randomly misoriented polycrystalline aggregates of cubic metals [10].
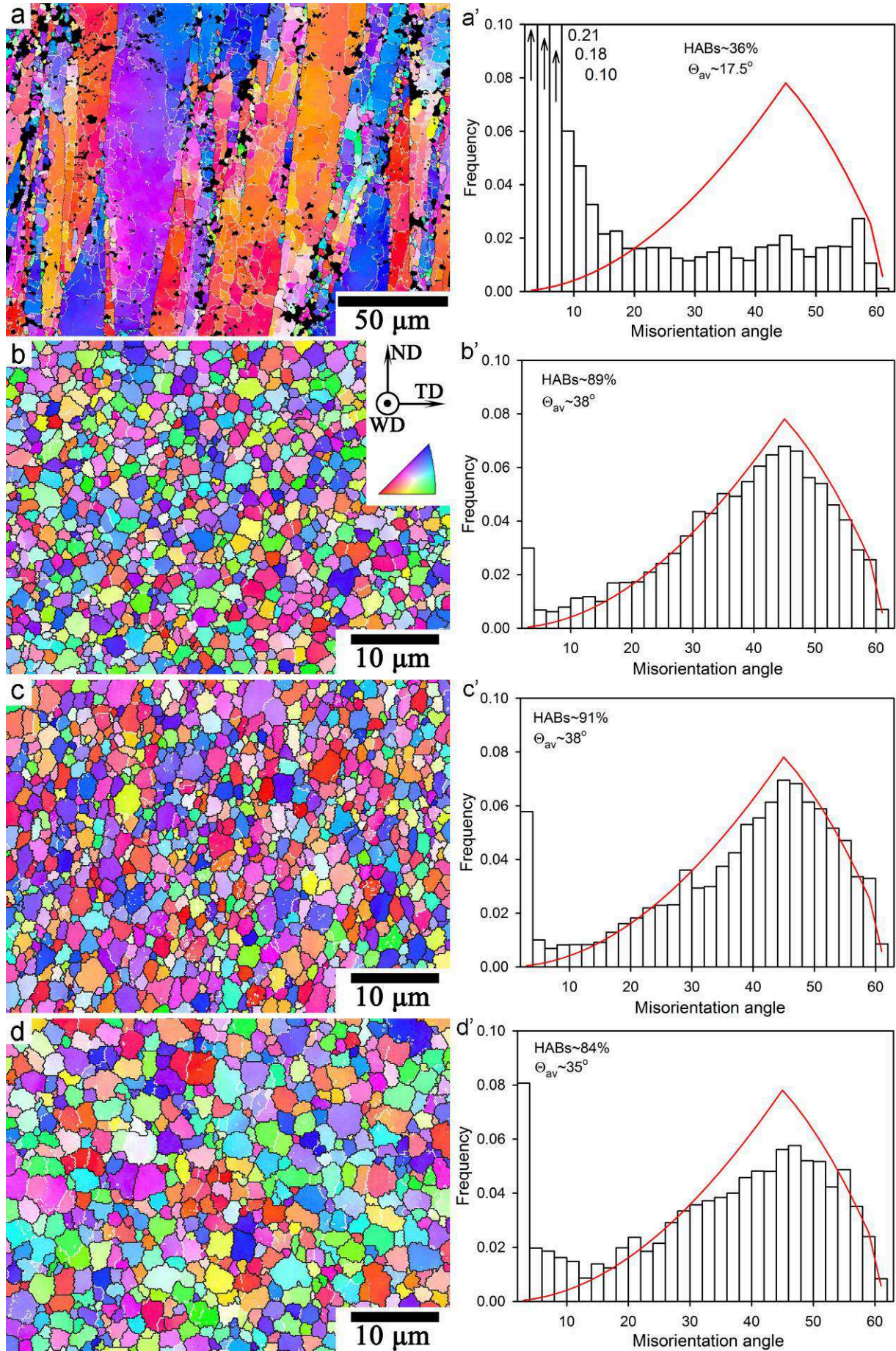
Fig. 2. The EBSD maps of 5024 alloy in as-received state (a, a') and subjected to FSW at 500 rpm (b, b'); 650 rpm (c, c'); 800 rpm (d, d')
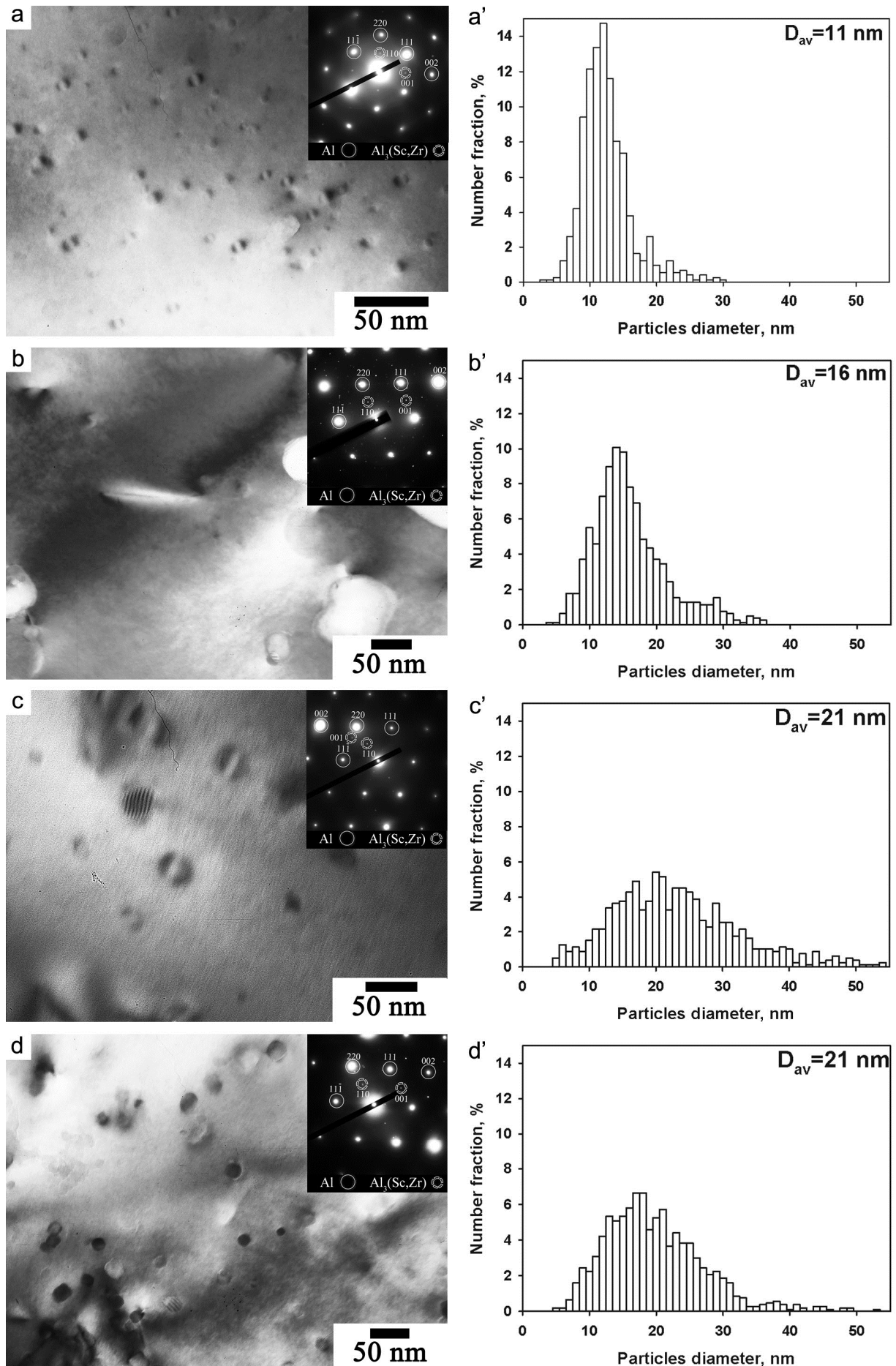
Fig. 3. TEM micrograph (a-d) and size distribution of Al$_3$(Sc,Zr) precipitates (a'-d') in as-received state (a, a') and subjected to FSW at 500 rpm (b, b'); 650 rpm (c, c'); 800 rpm (d, d')

Insignificant difference the theoretical value [10] and experimental date may be attributed to the formation of minor fraction of low-to-moderate boundaries. Increasing tool rotation speed to 800 rpm leads to increased grain size and remarkable deviation of misorientation distribution of theoretical function [10]. Dislocation density of $3 \div 4 \times 10^{13}$ m^{-2} is essentially independent on tool rotation speed (Table 1).

Table 1. Microstructural characteristics of materials FSW treatment

Tool rotation speed, [rpm]	Mean grain diameter, [μm]	HABs fraction, [pct.]	Average misorientation angle, [^{0}]	Dislocation density, [m^{-2}]	Mean diameter of Al$_3$(Sc,Zr) dispersoids, [nm]
-	200/20	36	17.5	~1×10^{13}	11
500	1.5	89	38	3×10^{13}	16
650	1.5	91	38	4×10^{13}	21
800	2.0	84	35	3×10^{13}	21

Effect of FSW on particles. Figure 3(a) shows typical TEM micrographs and distribution of dimensions of Al$_3$(Sc,Zr) dispersoids. These dispersoids demonstrating a well-known "coffee-bean" like contrast, which can be attributed to the coherent interface exerting a large coherent stress [14] exhibits a round shape and are uniformly distributed within the matrix. Hence, these dispersoids can be unambiguously recognized as coherent β'– phase (L12–Al$_3$(Sc,Zr)). The diffraction patterns shown in Figure 3 are indicative for existence of typical {100} and {110} superlattice reflections of the L12 structure and cube-cube orientation relationship (OR), supporting coherence/semi-coherence interfaces of the particles. The particle diameters distribution is characterized by sharp peak at 11 nm in initial material (Fig. 3(a')). The nano-scale Al$_3$(Sc,Zr) precipitates retain under FSW but their size increased from 11 nm to 16~21 nm (Fig. 3(b'-d'), Table 1). However, this size is below the critical diameter for Al-Mg-Sc alloys of 71 nm, at that the particles loss their coherency [12]. Indeed, diffraction analysis showed that OR between Al$_3$(Sc,Zr) and aluminum matrix of {111}$_{Al}$||{111}$_{β'}$ ⟨100⟩$_{Al}$|| ⟨100⟩$_{β'}$ (see the top right corners of Fig. 3 b-d) retains completely under FSW. This result confirmed the retaining coherent/semi-coherent nature of these precipitates in the stir zone. It is worth noting that along with superstructural spots a numerous small reflexes arranged randomly were observed, but their identification was failed.

It is worth noting that the Al$_3$(Sc,Zr) particles with dimension ≥20 nm may lose their coffee-been contrast. Therefore, FSW leads to a decrease in coherent stress that may affect mechanical properties. At the same time the Zener drag force originated from these particles is high enough to suppress both continuous and discontinuous grain coarsening. As a result, a very uniform UFG structure evolves in stir zones in the Al-Mg-Sc-Zr alloy. Friction heating dependent on tool rotational speed slightly affects the size of recrystallized grains, only.

Summary

FSW was demonstrated to be feasible for producing defect-free welds in the 5024 alloy. FSW produced a fully recrystallized structure with micron-scale grains (less 2 μm) in the stir zone. Nano-scale Al$_3$(Sc,Zr) dispersoids were found to tend for coarsening in the stir zone from 11 to 21 nm and part of then loss "coffee-bean" like contrast.

Acknowledgment

References

[1] Y. Estrin, A. Vinogradov, Extreme grain refinement by severe plastic deformation: A wealth of challenging science, Acta Mater. 61 (2013) 782-817.

[2] Z. Ma, F. Liu, R. Mishra, Superplastic deformation mechanism of an ultrafine-grained aluminum alloy produced by friction stir processing, Acta Mater. 58 (2010) 4693-4704.

[3] S. Malopheyev, V. Kulitskiy, S. Mironov, D. Zhemchuzhnikova, R. Kaibyshev, Friction-stir welding of an Al-Mg-Sc-Zr alloy in as-fabricated and work-hardened conditions, Mater. Sci. Eng. A 600 (2014) 159-170.

[4] X. Sauvage, A. Dede, A. Cabello Munoz, B. Huneau, Precipitate stability and recrystallisation in the weld nuggets of friction stir welded Al–Mg–Si and Al–Mg–Sc alloys, Mater. Sci. Eng. A 491 (2008) 346-371.

[5] P. Threadgill, A. Leonard, H. Shercliff, P. Withers, Friction stir welding of aluminium alloys, Int. Mater. Rev. 54 (2009) 49-93.

[6] R.S. Mishra, Z.Y. Ma, Friction Stir Welding and Processing, Mater. Sci. Eng. R 50 (2005) 1–78.

[7] Y. Sato, M. Urata, H. Kokawa, Parameters controlling microstructure and hardness during friction-stir welding of precipitation-hardenable aluminum alloy 6063, Metall. Mater. Trans. A 33 (2002) 625-635.

[8] J. Røyset, N. Ryum, Scandium in aluminium alloys, Inter. Mater. Rev 50 (2005) 19-44.

[9] A. Mogucheva, E. Babich, B. Ovsyannikov, R. Kaibyshev, Microstructural evolution in a 5024 aluminum alloy processed by ECAP with and without back pressure, Mater. Sci. Eng. A 560 (2013) 178-192

[10] J.K. Mackenzie, Second Paper on Statistics Associated with the Random Disorientation of Cubes, Biometrika 45 (1958) 229-240.

[11] D.B. Williams, C.B. Carter, editors. Transmission electron microscopy, New York, Plenum Press, 1996.

[12] S. Iwamura, Y. Miura, Loss in coherency and coarsening behavior of Al_3Sc precipitates, Acta Mater. 52 (2004) 591-600.